Comparison of Experimental Results with Thermodynamic Equilibrium Simulations of Supercritical Water Gasification of Concentrated Ethanol Solutions with Focus on Water Splitting

Julian Dutzi,* Athanasios A. Vadarlis, Nikolaos Boukis, and Jörg Sauer

ABSTRACT: Supercritical water gasification (SCWG) is a process in which biomass reacts with supercritical water to produce H_2 and CH_4-rich gas. The water-to-biomass ratio is a crucial variable in SCWG that affects the energy efficiency of the process. Despite the clear concept, systematic studies on water consumption during the formation of gaseous products are lacking. This study aims to determine the water consumption in SCWG of organic feedstock. Ethanol was used as an organic model compound since mass balances of complex biomasses like lignocelluloses are often incomplete due to the formation of solid deposits. The ethanol concentration ranged from 1.2 to 72 wt %, and complete gasification was achieved in all cases. Water consumption decreased with an increase in ethanol concentration due to enhanced methanation reactions with increasing organics. Stoichiometric calculations and ASPEN HYSYS simulations confirmed the experimental results, showing equilibrium gas compositions in the reaction system.

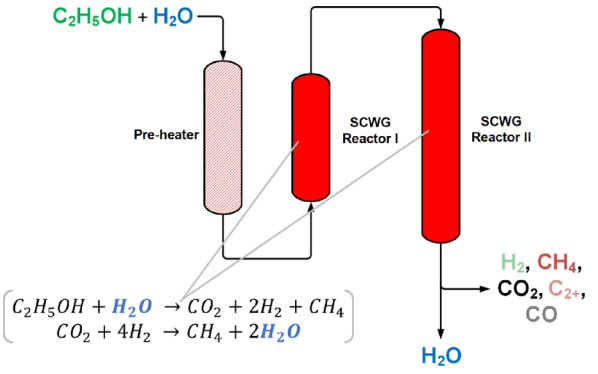

1. INTRODUCTION

The need for renewable energy and especially for hydrogen as an energy carrier is growing as carbon neutrality needs to be reached while an increasing need of energy needs to be covered. There are various production methods for green hydrogen, including water electrolysis using renewable energy sources, reforming of biogas, and biomass gasification.

One promising pathway for producing green hydrogen is through the gasification of biomass in supercritical water. Supercritical water gasification (SCWG) is a method that utilizes water as a reaction medium to convert organics into gaseous products with high efficiency. The process involves heating water (the main component of the feed) to temperatures and pressures at which it becomes supercritical.[1] This allows for excellent miscibility with the organic feedstock, resulting in fast and homogeneous reactions.[2] The process efficiency and the composition of the produced gas in SCWG are dependent on various process parameters, including temperature, pressure, and organic feed concentration.[3−8] Organic molecules are first hydrolyzed (eqs 1 and 2) and then further decomposed into gases followed by the water gas shift reaction (eq 3) and methanation reactions (eqs 4 and 5).[9−11]

The process of SCWG yields a gas mixture that primarily comprises H_2, CH_4, and CO_2, while C_2 and C_3 compounds and CO are present in low quantities.[12−16] Moreover, the gas produced through SCWG is already compressed, eliminating the need for further compression during subsequent gas synthesis or storage.[15,17,18]

$$C_xH_yO_z + (2x - z)H_2O \rightarrow xCO_2 + (2x - z + 0.5y)H_2 \quad (1)$$

$$C_xH_yO_z + (x - z)H_2O \rightarrow xCO + (x - z + 0.5y)H_2 \quad (2)$$

$$CO + H_2O \leftrightarrow CO_2 + H_2 \quad (3)$$

$$CO + 3H_2 \leftrightarrow CH_4 + H_2O \quad (4)$$

$$CO_2 + 4H_2 \leftrightarrow CH_4 + 2H_2O \quad (5)$$

As displayed in eqs 1 to 5, water plays an important role as a reactant in the SCWG. Until now, the amount of water that reacts to form gaseous products within the process has received little interest and has not been systematically studied. The water-to-biomass ratio in the feed influences the process in terms of gasification efficiency[19−21] and is an important factor on the SCWG energy efficiency and economics.[22,23]

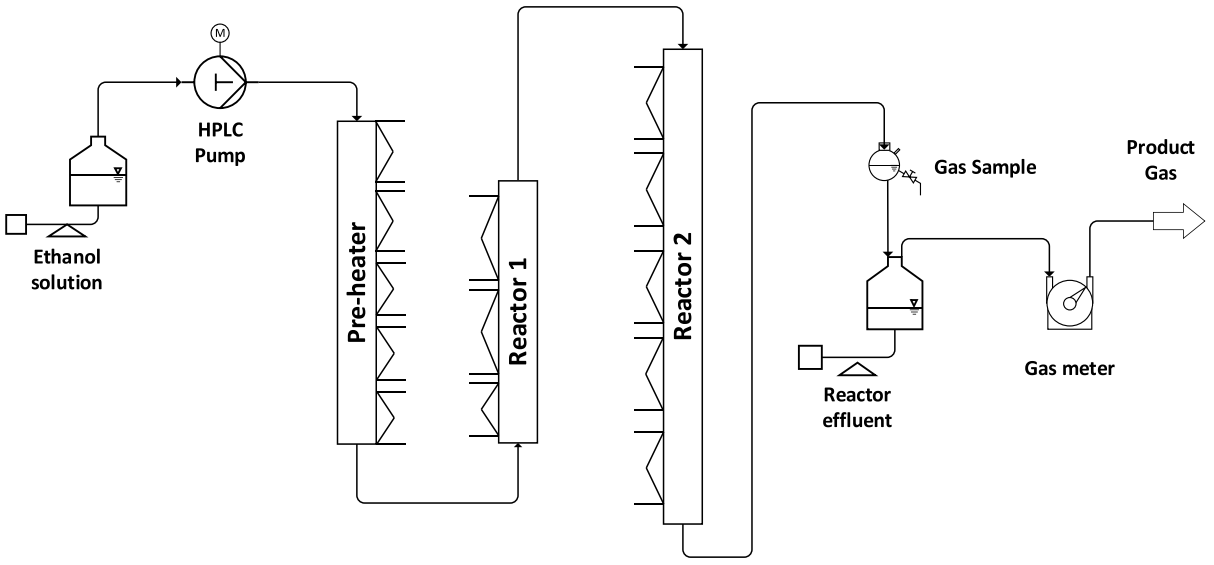

Figure 1. Schematic diagram of the LENA plant in the present configuration.

Fiori et al. simulated the SCWG process of different biomasses and calculated the water consumption of 10 wt % glycerol solution to be 22.5 kg h^{-1} when processing 1000 kg h^{-1} solution (T = 700 °C, p = 300 bar).[24] Wang et al. simulated the catalytical SCWG of lignin on a molecular scale and calculated the water consumption as a function of total water molecules present in the system.[25] In the following work, the influence of the biomass concentration, conducted with the model component ethanol, on the water consumption of the SCWG is experimentally investigated and theoretically described. Additionally, the experimental data is compared to an ASPEN HYSYS simulation. The results of these experiments provide valuable insights into the process of supercritical water gasification of ethanol and can be transferred to the conversion of real biomass. The results are complemented with a study on the influence of potassium as a catalyst on the reaction system. It is important to understand the influence of homogeneous catalysts on the process, not only in terms of chemistry[26,27] but also in terms of how they alter the reaction system (e.g., the reactor walls) permanently.[28,29]

2. MATERIALS AND METHODS

2.1. Preparation of Educts. Pure ethanol is mixed with distilled water at concentrations of 1.2 to 72 wt % to create the feed solution. The ethanol is supplied by VWR Chemicals. When needed, $KHCO_3$ is added as a catalyst.

2.2. Apparatus. At the Karlsruhe Institute for Technology, laboratory SCWG tests are conducted in the Laboratory Plant for Energetic Utilization of Agricultural Materials, abbreviated as LENA (German acronym). LENA is a high-pressure plant that operates at temperatures of up to 700 °C and pressures of up to 30 MPa. The reaction system comprises a preheater and two gasification reactors (as shown in Figure 1).

The preheater, which is made of a nickel-based Inconel 625 alloy, has an inner diameter of 8 mm and a length of 1200 mm. Five electric spiral heaters heat the preheater from the outside, with two thermocouples attached to the outer wall of the pipe for each heater. In the preheater, the supercritical state of water is achieved.

The gasification reactors are made of Inconel 625 and have lengths of 1100 and 1800 mm and an inner diameter of 8 mm. Reactor 1 is heated from the outside by an electric spiral heater and three electric rod heaters. Seven thermocouples are mounted on the outer wall to monitor the temperature. Reactor 2 is heated by one electric spiral heater and six electric rod heaters, and nine thermocouples are mounted on the outer wall of the reactor for temperature monitoring.

Even though the thermocouples are only mounted on the outside of the reactor and are not in contact with the fluids, the outside temperature can be considered representative of the reaction temperature. D'Jesus investigated the temperature difference between outside and inside the reactor in a similar system with pure water and a biomass slurry (8 wt % biomass).[21] Little to none temperature deviation was noticed.

The reaction mixture is converted into gaseous products in the reactors. To quantify the products, gas meters (Ritter GmbH) and scales (Soehnle GmbH) are installed. During the experiment, liquid and gas samples are collected in regular intervals. The evaluation is based on the steady-state operating condition where the gas composition and gas production remain constant.

The system is pressurized by pumping water with a high-pressure pump by Prominent and then heated. In the process control system, the temperatures are set for this purpose. The ethanol solution is then pumped into the system with an HPLC pump. The pressure in the system is regulated by a back-pressure regulator by Tescom.

The LENA lab-plant is designed for the processing of real biomass.[30] For the gasification of ethanol solution, a simpler setup would also be sufficient.

2.3. Analysis. The gas chromatograph 5890 series II plus (Hewlett Packard Inc.) equipped with a fused silica capillary column (Carboxen 1010 PLOT 30 m, SUPELCO) is used to analyze gas samples of the product gas. The thermal conductivity and flame ionization detectors are used to determine the volume fractions of gas components including H_2, CO, CH_4, CO_2, C_2H_4, C_2H_6, C_3H_8, and C_3H_6. Gas samples are collected every 30 min for analysis.

The total carbon (TC) and total inorganic carbon (TIC) in liquid samples during the experiment and in the total effluent are determined by combustion and acid extraction, respectively, using a TOC-analyzer (DIMATOC 2100, DIMATEC).

Total organic carbon (TOC) is calculated by subtracting TIC from TC. The concentration of trace elements (Al, Ca, Cr, Cu, Fe, K, Mg, Mo, Na, Ni, S, Si, and Zn) is measured using an Agilent 725 spectrometer via ICP-OES (inductively coupled plasma-optical emission spectrometry).

2.4. Data Interpretation. For the data interpretation, the ethanol mass fraction w_{EtOH} (eq 6) and the ratio of carbon to water in the feed x_c^* (eq 7) are used:

$$w_{EtOH} = \frac{\dot{m}_{EtOH}}{\dot{m}_{EtOH} + \dot{m}_{H_2O}} \tag{6}$$

where $\dot{m}_i$ is the mass flow of species "i" (g/h)

$$x_c^* = \frac{\dot{n}_C}{\dot{n}_{H_2O}} = \frac{2\dot{n}_{EtOH}}{\dot{n}_{H_2O}} \tag{7}$$

where $\dot{n}_i$ is the molar flow of species "i" (mol/h).

The following section describes the key figures, the carbon gasification yield (CE), the total organic carbon conversion (TOC-conversion), and the water consumption (WC) of the process.

The CE represents the proportion of carbon in the feed that is transferred to the gas phase and thus is a key figure that describes how well the organics in the feed solution are gasified. The properties of gases are approximated by the ideal gas law. CE is calculated as follows:

$$CE = \frac{\sum \beta_i \times x_i \times \frac{\dot{V}_{Gas} \times p}{R \times T} \times M_c}{\dot{m}_{Feed} \times \alpha} \tag{8}$$

where x_i is the concentration of component "i" in the gas product (vol %), α is the carbon concentration in the feed (wt %), β_i is the number of carbon atoms of component "i" in the gas product, $\dot{m}_{Feed}$ is the feed mass flow (g/h), M_c is the molar mass of carbon (g/mol), p is the pressure (Pa), R is the universal constant of gases, T is the temperature (K), and $\dot{V}_{Gas}$ is the gas flow under ambient conditions (L/h).

The TOC-conversion measures the proportion of the TOC in the feed slurry that is converted into other forms, including gases, dissolved inorganic compounds, and organic residue (coke, tar, and soot), and thus, the TOC-conversion is an important indicator of the quality of the wastewater, and it is defined as follows:

$$TOC - conversion = 1 - \frac{\dot{m}_{R,effluent} \times TOC_R}{\dot{m}_{Feed} \times \alpha} \tag{9}$$

where $\dot{m}_{R,\ effluent}$ is the mass flow of the reactor effluent (g/h) and TOC_R is the TOC content of the reactor effluent (mg/g).

The water consumption of the process describes how much water is converted into gaseous products when reacting with the organic compounds. In previous studies, it was shown that the reactor effluent of the SCWG process can be recycled.[21,30] The water consumption is thus important for the estimation of how much fresh water needs to be used to make up for the difference of water in feed and reactor effluent by distilled water and thus is important for cost estimation of the SCWG process. To calculate the generation of H_2 and CH_4 from water, the amount of C, H, and O in the gas phase is compared with the amount of C, H, and O that originate from the gasified ethanol $\dot{n}_{EtOH,\ gasified}$.

$$\dot{n}_{EtOH,gasified} = CE \times \dot{n}_{EtOH,Feed} \tag{10}$$

where $\dot{n}_i$ is the molar flow of species "i" (mol/h).

Any additional H and O (ΔH and ΔO (eqs 12 and 13)) in the product gas have its origin in water that has reacted with the ethanol since those are the only two components that are fed into the system (except for $KHCO_3$, which is present in neglectable amounts and is assumed to leave the system also in form of $KHCO_3$ and thus does not contribute to gas formation).

$$\Delta C = \dot{n}_{CH_4} + \dot{n}_{CO} + \dot{n}_{CO_2} + 2\dot{n}_{C_2H_4} + 2\dot{n}_{C_2H_6} + 3\dot{n}_{C_3H_6} + 3\dot{n}_{C_3H_8} - 2\dot{n}_{EtOH,gasified} \tag{11}$$

$$\Delta O = \dot{n}_{CO} + 2\dot{n}_{CO_2} - \dot{n}_{EtOH,gasified} \tag{12}$$

$$\Delta H = 4\dot{n}_{CH_4} + 2\dot{n}_{H_2} + 4\dot{n}_{C_2H_4} + 6\dot{n}_{C_2H_6} + 6\dot{n}_{C_3H_6} + 8\dot{n}_{C_3H_8} - 6\dot{n}_{EtOH,gasified} \tag{13}$$

where Δj is the molar difference of element "j" (mol/h).

ΔC is zero since all carbon in the gaseous phase originates from gasified ethanol. Since the differences in H and O in real experiments show little deviations to the elemental composition of water, the mean value of these differences ΔO and ΔH is used to calculate the water consumption WC relative to the processed amount of ethanol according to the following equation:

$$WC = \frac{0.5\Delta H + \Delta O}{2} \times \frac{1}{\dot{n}_{EtOH,gasified}} \frac{mol\ H_2O}{mol\ C_2H_5OH} \tag{14}$$

3. RESULTS AND DISCUSSION

To investigate the influence of the reactor wall on the supercritical water gasification of ethanol and the effect of potassium as a catalyst, three long-time experiments (operation >19 h) were conducted (see Table 1). The reaction temperature was 650 °C, and the pressure was 28 MPa. The set mass flow was 250 g h^{-1}.

Table 1. Conditions of Long-Time Ethanol Experiments

Exp. Nr.	feed	w_{EtOH} (wt %)	K^+ (ppm)	duration (h)
1	ethanol solution	6		46
2	ethanol solution + $KHCO_3$	6	100	25
3	ethanol solution	5		19

In a second set of experiments, the water consumption of the SCWG process was investigated for different ethanol concentrations (see Table 2). The reaction temperature was 650 °C, and the pressure was 28 MPa. The set mass flow was 250 g h^{-1}.

3.1. Long-Time Ethanol Experiments. It is well known from the literature that the elemental composition of the surface of the reactor wall affects the supercritical water gasification of organics.[31,32] Boukis et al. discovered that pre-oxidizing the reactor walls (Alloy 625) with H_2O_2 solution oxidized the nickel in the alloy to form NiO, which can later be reduced to metallic Ni, and also reduced organic impurities (C and N) on the surface.[31] This resulted in a catalyzed WGS reaction and therefore in a significantly lower CO yield. To investigate if a modification of the reactor wall appears during

Table 2. Conditions of Ethanol Experiments with Variation of Concentration

Exp. Nr.	feed	w_{EtOH} (wt %)	x_c^* (mol/mol)	K^+ (ppm)
4	ethanol solution + $KHCO_3$	1.2	0.01	100
5	ethanol solution + $KHCO_3$	6.0	0.05	100
6	ethanol solution + $KHCO_3$	11.5	0.1	100
7	ethanol solution + $KHCO_3$	20.0	0.2	100
8	ethanol solution + $KHCO_3$	30	0.34	100
9	ethanol solution + $KHCO_3$	39	0.5	100
10	ethanol solution + $KHCO_3$	56	1	100
11	ethanol solution + $KHCO_3$	72	2	100

long-time processing of ethanol without pre-oxidizing the reactor walls, ethanol solution (6 wt % ethanol) was gasified in a newly implemented reaction system that had not been used for any other experiments beforehand (experiment 1).

After reaching a steady state, the gas composition did not change until the end of the 46 h long experiment (see Figure 2). The mean gas composition is displayed in Figure 3. According to Arita et al., ethanol first gets stripped of a H_2 molecule and afterward is equally separated into CH_4 and CO in terms of moles.[32] CO then reacts further with water according to the WGS reaction to form H_2 and CO_2. This explains that H_2 and CH_4 make up the biggest part of the produced gas. Besides this, a dehydration reaction of ethanol to form C_2H_4 takes place. By reacting with a H_2 molecule, C_2H_6 is formed. Since the CO concentration stayed at about 12% over the course of the 46 h, it can be assumed that the reactor wall was not modified in such a way that more NiO and Ni were present that could enhance the WGS reaction. Thus, to further promote the WGS reaction, the reactor wall either needs to be pretreated or catalysts that enhance the reaction need to be added.

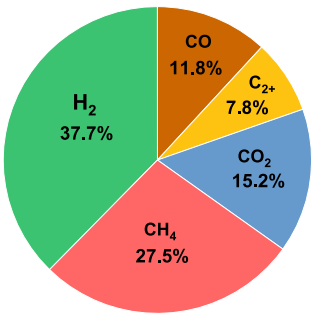

Figure 3. Mean gas composition of gasification of ethanol in vol % (experiment 1).

Over the course of the experiment, two balancing intervals are set, in which gas and liquid samples were taken (interval 1: 19.8−29.1 h; interval 2: 43.5−46.5 h). As the experiment progressed, further less gas was produced, as can be seen in Figure 4.

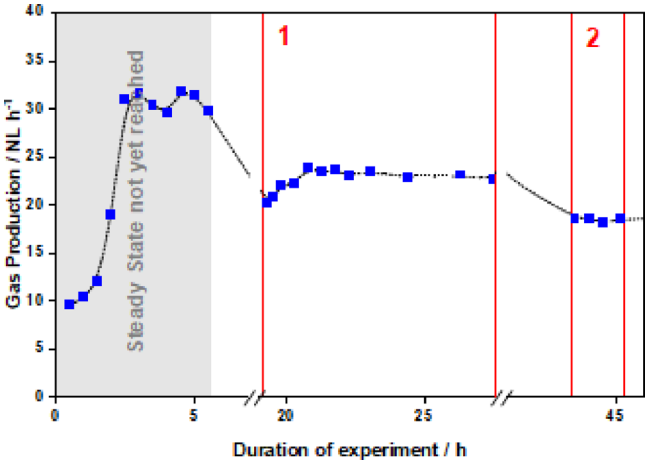

Figure 4. Gas production of the gasification of ethanol with two defined evaluation periods (experiment 1).

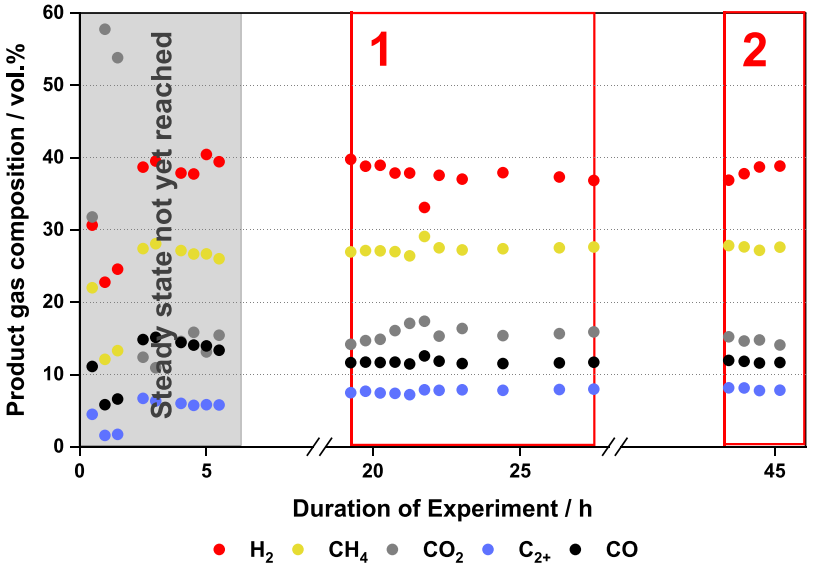

Figure 2. Gas composition of the gasification of ethanol with two defined evaluation periods (experiment 1).

In interval 1, 1.55 L $g_{Ethanol}^{-1}$ of gas was produced, while in interval 2, only 1.25 L $g_{Ethanol}^{-1}$ was produced (see Table 3).

Table 3. Evaluation of the Balance Intervals (Experiment 1)

balancing interval	1	2
duration of experiment (h)	19.8–29.1	43.5–46.5
mass balance (%)	101.70	96.55
C-balance (%)	113.83	91.01
CE (%)	113.56	90.75
TOC-conversion (%)	100.00	99.88
gas production ($NL/g_{Ethanol}$)	1.55	1.25

At the same time, the carbon efficiency (CE) and the carbon mass balance decreased by about 23%. A possible reason for this could be the enhanced coke formation over time. Due to heavy coke formation, a filter had to be installed prior to the pressure regulator to ensure long-time operation without plugging of the pressure regulator (see Figure 5).

Figure 5. Reactor effluent sample taken without and with filter installed (experiment 1).

Heavy coke formation was also observed by Diem et al. when gasifying ethanol solutions.[33] Therdthianwong et al. proposed that the formation of carbonaceous species, like coke, follows the cracking of hydrocarbons (eqs 16 and 17) and the Boudouard reaction (eq 15) at high temperatures (T = 600 °C):[34]

$$2CO \rightarrow C + CO_2 \quad \Delta H^0_{298K} = -172 \frac{kJ}{mol} \tag{15}$$

$$CH_4 \rightarrow C + H_2 \quad \Delta H^0_{298K} = 75 \frac{kJ}{mol} \tag{16}$$

$$C_nH_m \rightarrow nC + \frac{m}{2}H_2 \tag{17}$$

Enhanced coke formation could explain the reduced carbon efficiency and C-balance since the coke cannot be collected during the experiment and therefore cannot be calculated into the steady-state C-balance. Coke formation also poisons the catalytically active metals in the reactor wall.[33] This further reduces active Ni sites on the reactor wall and can explain the data in Table 3.

Over the course of experiment 1, the pH of the liquid effluent decreased from 6.4 to 3.6 (see Supporting Information Table S1). A possible reason for this could be an increased amount of CO_2 that is dissolved in the effluent. With increasing CO_2 content in the effluent, the pH drops (eq 18).[35]

$$CO_2 + H_2O \rightarrow HCO_3^- + H^+ \tag{18}$$

The dissolved CO_2 is not measured by the gas meter, and thus this could be another reason for the decreasing gas production over time.

As mentioned above, the content of CO in the product gas did not change during SCWG with 6 wt % ethanol (experiment 1). To demonstrate the effect of homogeneous catalysts, potassium (100 ppmw) was added in the form of $KHCO_3$. It is well known from the literature that homogeneous catalysts such as K_2CO_3 or KOH increase the gasification yield and enhance the WGS reaction.[36−41] Sinăg et al. have found that the H_2 yield doubles when K_2CO_3 is used compared to the operation without a catalyst for gasification of glucose.[36] Their proposed reaction mechanism (taken from Sinăg et al.[36]) adjusted for the used salt in this study $KHCO_3$ is the following (eqs 19–22):

$$2KHCO_3 \rightarrow K_2CO_3 + H_2O + CO_2 \tag{19}$$

$$K_2CO_3 + H_2O \rightarrow KHCO_3 + KOH \tag{20}$$

$$KOH + CO \rightarrow HCOOK \tag{21}$$

$$HCOOK + H_2O \rightarrow KHCO_3 + H_2 \tag{22}$$

Directly after experiment 1 (without stopping the lab-plant), 100 ppmw K^+ was added to the ethanol solution (start of experiment 2) (see Figure 6, start of adding K^+ at t = 0 h).

The H_2 concentration increased rapidly from 38 to 55 vol %, CO_2 also increased by about 7 vol % from 16 to 23 vol %. The concentration of CO significantly dropped from 12 to 0.5 vol %. Thus, the WGS reaction is significantly catalyzed, as expected. The CH_4 formation is also limited since the reaction of CO to CH_4 is reduced due to the low CO content. The addition of potassium also limits the formation of coke.[33,36,40] This can be seen by comparing CE and the C-balance prior and after adding K^+. Both increased by about 6% compared to interval 2 to 96.8%.

Interestingly, the addition of $KHCO_3$ seems to have permanently altered the reaction system. This can be seen by looking at the gas composition of experiment 3 (see Figure 7). Before this experiment, the system was cleaned with water and the experiment itself was conducted without the addition of $KHCO_3$ but the gas composition is roughly the same as during the experiment with $KHCO_3$. The WGS is still being catalyzed even though no homogeneous catalyst is present anymore. Additionally, this experiment could be conducted without any filter installed since no coke formation was noticeable. This could be due to the changes in the surface of the reactor walls after being exposed to $KHCO_3$ during experiment 2. Although the inner surface of the present reactor was not analyzed, it is well known that potassium carbonates cause corrosion in the nickel-alloy Inconel 625 under the conditions of SCWG,[28,29,42−47] with corrosion rates increasing at temperatures above 500 °C.[29] Without addition of potassium carbonates, no remarkable corrosion was visible during the gasification of 5 wt % methanol (p = 240 bar, T = 600 °C).[42] The reactor surface is thus permanently altered after the application of potassium carbonates, resulting in areas rich in NiO.[29] Like during experiment 1, the pH showed a slight decrease during operation with $KHCO_3$ (pH = 5.6, sample

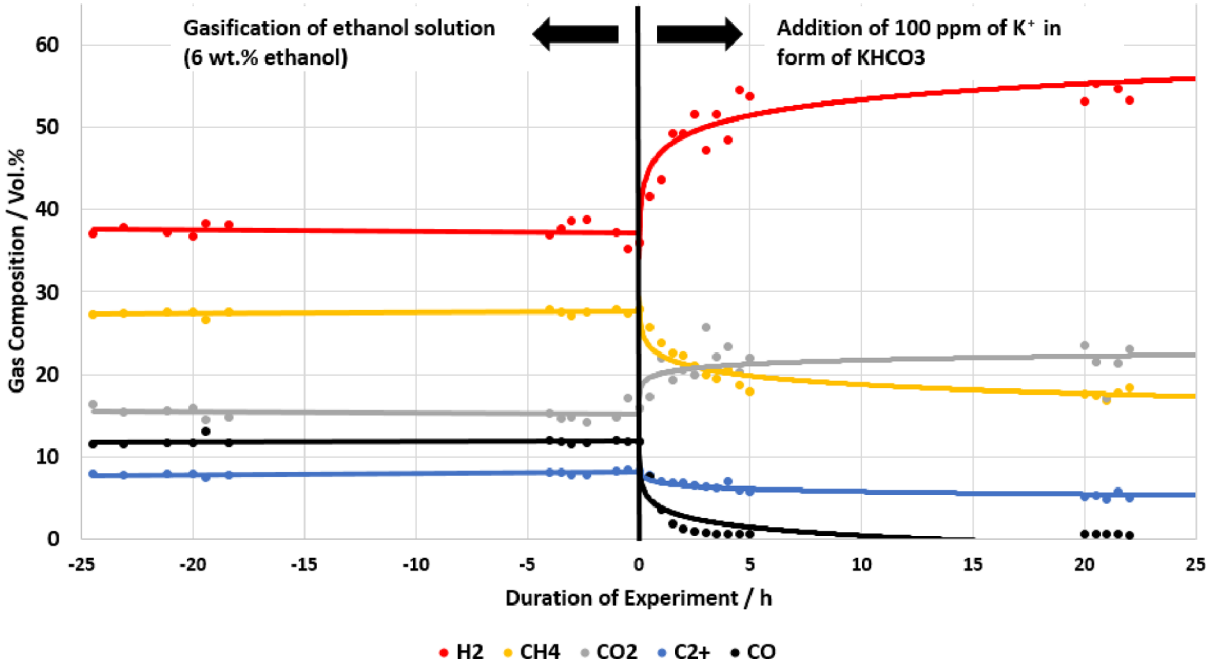

Figure 6. Change of gas composition after the addition of potassium (experiments 1 and 2) (line: linear regression due to stable operation in experiment 1, logarithmic regression in experiment 2).

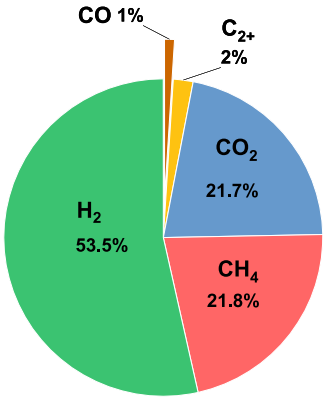

Figure 7. Gas composition of experiment 3 in vol %.

taken 2 h after addition of $KHCO_3$, pH = 6.2 after 3.5 h of operation with $KHCO_3$, pH = 4.2 after 20 h of operation).

One significant change in the gas compositions of experiments 2 and 3 is the drop in higher hydrocarbons from 7 to 2 vol %. During experiment 2, a slow decrease in the concentration of C_{2+} compounds could be detected. The cause of this is unknown. By the addition of potassium, the dehydrogenation of ethanol to form hydrocarbons seems to be inhibited. The fact that C_{2+} compounds are of low concentration when adding $KHCO_3$ was also observed by Diem et al.[33] In the present case, it is interesting that the concentration stays low even though no catalyst was added anymore.

3.2. Investigation of Water Consumption. Eight experiments were conducted to investigate the water consumption during the SCWG of different ethanol solutions (100 ppm K^+ was added) (see Table 2 and Table 4).

In all experiments conducted, the TOC conversion was greater than 99%. The carbon efficiency was greater than 95.5% in all cases except for $x_c^* = 0.01$ (see Table 4), and thus, the gasification can be considered complete for all concentrations. Since TOC-conversion is complete and no solid carbon was found for $x_c^* = 0.01$, the relatively low CE is most likely due to uncertainties of the measurement (especially the gas meter), which have a greater impact if the gas flow is low.

This is surprising since CE is generally known to decrease with increasing concentration of organics.[20,21] In the present reactor configuration, ethanol could be gasified effectively even at high concentrations. The temperatures (T = 650 °C) and residence times (calculation based on the density of water) at T > 600 °C (τ = 3 min) are high for the conversion of ethanol. For high feed concentrations of ethanol, the density of the

Table 4. Key Figures of Gasification of Different Ethanol Solutions

Exp. Nr.	w_{EtOH} (wt %)	x_c^* (mol/mol)	CE (%)	TOC-conversion (%)	mass balance (%)	carbon balance (%)	amount of gas (L g_{EtOH}^{-1})
4	1.2	0.01	93.6	99.42	99.2	93.6	2.84
5	6.0	0.05	97.6	99.94	98.4	96.7	2.26
6	11.5	0.10	95.9	99.98	101.8	94.5	1.7
7	20.0	0.20	95.6	99.99	98.5	95.6	1.38
8	30.0	0.34	98.2	100.00	99.2	98.2	1.24
9	39.0	0.50	96.6	100.00	96.9	96.6	1.16
10	56.0	1.00	96.2	100.00	96.4	96.3	1.06
11	72.0	2.00	96.5	99.95	98.0	96.6	1.01

mixture decreases and thus the residence time will decrease. Since complete gasification is reached in all cases, the change in residence time has no impact on the process under the chosen conditions. Byrd et al. studied the SCWG of ethanol over a Ru(5 wt %)/Al_2O_3 catalyst and demonstrated the significant effect of residence time and of temperature on the yield of products and gasification.[48] More specifically, at 600 °C and low residence time (5 s), they detected high amounts of organic carbon in the liquid effluents and increased ethylene yield. When they increased the residence time to 10 s, these products were minimized, while the yields of H_2, CH_4, and CO_2 increased significantly. Voll et al. calculated the thermodynamic equilibrium of ethanol SCWG and compared their results with Byrd et al.[48,49] They argued that a minimum residence time of 4 s results in satisfactory results when it comes to ethanol SCWG. The ethanol decomposition in supercritical water is known to already take place at 500 °C.[32] Since these two factors positively influence the gasification efficiency,[13,50−56] the high temperature and residence time could explain why complete gasification could be reached for ethanol concentrations up to 72 wt %.

From the literature, it is well known that the concentration of the organic components significantly influences the composition of the product gas of the SCWG process. With rising organic content, the water surplus decreases, which reduces the amount of H_2 produced.[19,20,57] The CH_4 was found to increase with rising organic concentration.[57,58] In the case of ethanol, the methane could originate from methanation or acetaldehyde decarbonylation. Both described effects could be already seen in the present study (see Figure 8).

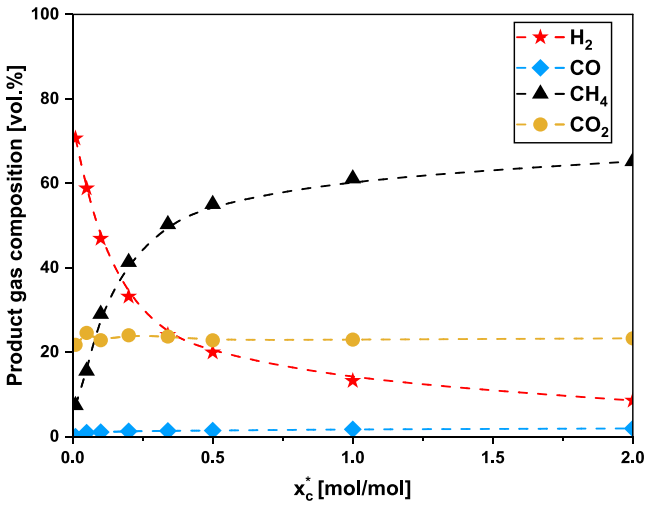

Figure 8. Influence of x_c^* in the feed solution on the composition of the product gas.

The H_2 content of the product gas decreased from 70.1 to 8.5 vol % when increasing the ethanol concentration from 1.2 to 72 wt % (x_c^* 0.01 to 2 mol/mol). The CO concentration remained below 2 vol % with little increase. An increase with rising organic concentration is expected due to the reverse water-gas shift reaction.[20,59] As described in Section 3.1, once potassium is present in the system, almost no CO is produced due to the significantly enhanced water-gas shift reaction.[36] It is demonstrated that 100 ppm potassium is sufficient to enhance the reaction to such an extent that even with an ethanol concentration of 72 wt %, almost no CO is detectable. When increasing the feed concentration, the CH_4 content of the product gas rose from 7.1 to 65.2 vol %. The increased methane content correlates with the decrease in the amount of produced gas per gram ethanol gasified (from 2.84 to 1.01 L g_{EtOH}^{-1}) since according to reactions 4 and 5, four or five gas molecules react to form one molecule of methane and water. Since the gasification of ethanol solutions with 1.2 to 72 wt % was possible and, in all cases, complete (CE > 93.6%), it can be assumed that the same reaction mechanism can be applied for all concentrations. Since almost no higher hydrocarbons can be detected, the major reaction pathway can be described by dehydrogenation of ethanol, as proposed by Arita et al.[32]

$$C_2H_5OH \rightarrow H_2 + CH_3CHO \quad (23)$$

$$CH_3CHO \rightarrow CH_4 + CO \quad (24)$$

$$CO + H_2O \rightarrow CO_2 + H_2 \quad (25)$$

Subsequently, either steam methane reforming or methanation reactions (eqs 4 and 5) take place, which depend on the amount of water in the system and thus on the ethanol concentration. In the case of x_c^* = 0.01 and x_c^* = 0.05, the amount of methane in the product gas is significantly lower than the amount that forms according to eqs 23 and 24. In this case, steam methane reforming seems to be taking place. For higher x_c^* than 0.05, the amount of methane contained in the product gas can not only be explained by eqs 23 and 24 since the amount of methane in the product gas is greater than the amount of ethanol processed on molar base (see Table 5).

The methanation reaction and steam methane reforming thus directly influence the water consumption of the SCWG process since the formed water during methanation reduces the amount of water consumed. This effect can be seen in Figure 9 and Table 6. The water consumption decreases from 2.38 to 0.06 mol H_2O consumed per mol ethanol when increasing x_c^* from 0.01 to 2. At low x_c^*, the deviation of the measured water consumption to the water consumption given in eq 1 for ethanol (3 mol H_2O per mol ethanol) is the smallest. This deviation can be well explained by the formed methane. When further reducing the feed concentration, the water consumption of 3 mol H_2O per mol ethanol would then be the limit. It becomes clear that the higher the methane content of the product gas, the lower the water consumption of the process is.

To verify the proposed mechanism (eqs 23 to 25 and eqs 4 and 5), the following theoretical consideration was conducted. The proposed mechanism by Arita et al.[32] can be reduced to eq 26

$$C_2H_5OH + H_2O \rightarrow CO_2 + 2H_2 + CH_4 \quad (26)$$

$$CO_2 + 4H_2 \rightarrow CH_4 + 2H_2O5^*$$

Table 5. Ratio of Methane in the Product Gas to Ethanol in Feed for Different x_c^* Values

x_c^* (mol/mol)	0.01	0.05	0.1	0.2	0.34	0.5	1	2
n_{CH_4}/n_{EtOH} (mol/mol)	0.44	0.72	1.02	1.17	1.27	1.30	1.34	1.36

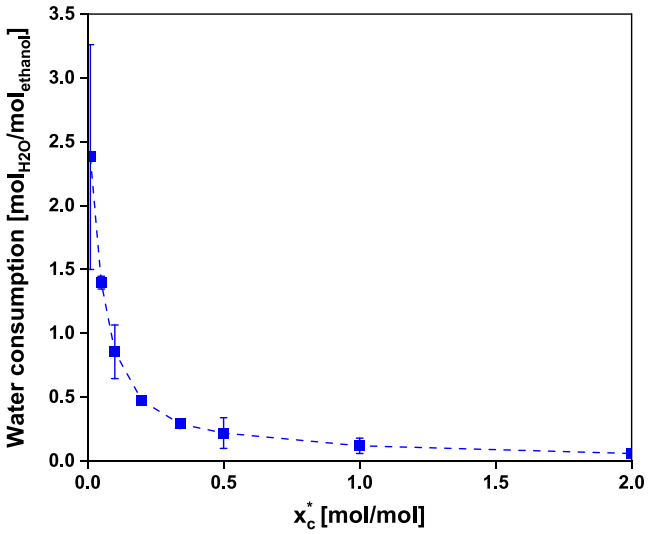

Figure 9. Water consumption of the SCWG process with variation in x_c^* in the feed solution.

When also taking the methanation into account (eq 5, for simplicity again displayed as eq 5*), the resulting gas composition (CO and higher hydrocarbons are neglected due to the small amount in the product gas) can thus be described by adding these equations. For this, eq 5* is multiplied by the factor x and eq 26 with the factor y

$$y C_2H_5OH + (y - 2x)H_2O \rightarrow (y - x)CO_2 + (2y - 4x)H_2 + (y + x)CH_4 \quad (27)$$

The water consumption WC can thus be described by the reduced formula ($y = n_{EtOH,\ gasified}$)

$$WC = \frac{n_{EtOH,gasified} - 2x}{n_{EtOH,gasified}} \frac{\text{mol } H_2O}{\text{mol EtOH}} \quad (28)$$

The produced amount of gas can be described as displayed in eqs 29 to 31:

$$n_{CH_4} = y + x = n_{EtOH,gasified} + x \quad (29)$$

$$n_{CO_2} = y - x = n_{EtOH,gasified} - y \quad (30)$$

$$n_{H_2} = 2y - 4x = 2n_{EtOH,gasified} - 4x \quad (31)$$

The variable "x" can thus be described in various ways

$$x = n_{CH_4} - n_{EtOH,gasified} = \frac{2n_{EtOH,gasified} - n_{H_2}}{4} = n_{EtOH,gasified} - n_{CO_2} \quad (32)$$

With this formula, the water consumption can be described as

$$WC = 3 - 2\frac{n_{CH_4}}{n_{EtOH,gasified}} = \frac{1}{2}\frac{n_{H_2}}{n_{EtOH,gasified}} = 2\frac{n_{CO_2}}{n_{EtOH,gasified}} - 1 \frac{\text{mol } H_2O}{\text{mol EtOH}} \quad (33)$$

To verify this theoretical consideration, the experimental data are displayed graphically and approximated with a linear regression (see Figure 10). As displayed, the received linear

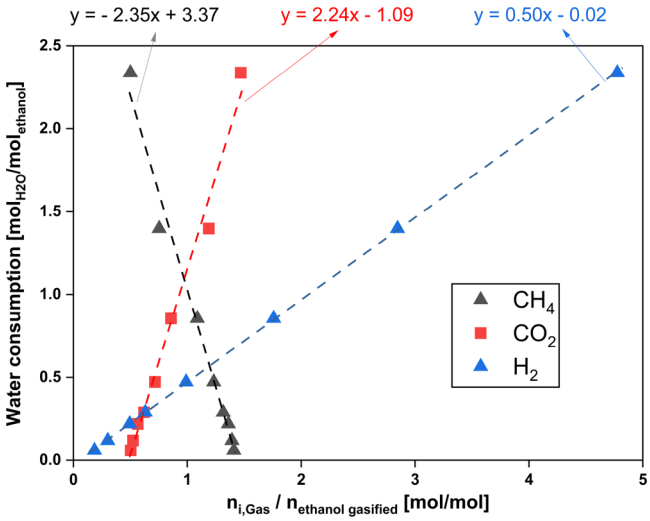

Figure 10. Water consumption as a function of the produced gases.

regressions fit the calculations of the theoretical water consumption well with a deviation smaller than 20%. The proposed reaction mechanism is thus justified.

3.3. Comparison of Experimental Results with Thermodynamic Equilibrium. The experimental results were additionally compared with the thermodynamic equilibrium calculated with Aspen HYSYS V14. The simulation was carried out with a Gibbs reactor, which minimizes the free Gibbs energy of the system. The selected property package was the PR-Twu implementing the equation of state (EOS) for enthalpy calculations. As stated by Twu et al., their

Table 6. Calculation of Water Consumption from Experimental Data (According to Equations 11−14)

			water consumption		
x_c^* (mol/mol)	ΔH (mol H/mol EtOH)	ΔO (mol O/mol EtOH)	based on ΔH (mol H_2O/mol EtOH)	based on ΔO (mol H_2O/mol EtOH)	mean (mol H_2O/mol EtOH)
0.01	5.64	1.94	2.82	1.94	2.38
0.05	2.74	1.42	1.37	1.42	1.40
0.1	1.91	0.75	0.96	0.75	0.86
0.2	0.95	0.47	0.48	0.47	0.47
0.34	0.61	0.28	0.31	0.28	0.29
0.5	0.55	0.16	0.28	0.16	0.22
1	0.30	0.09	0.15	0.09	0.12
2	0.14	0.05	0.07	0.05	0.06

temperature-dependent function for a cubic EOS correctly extrapolates the vapor pressures of pure components to the supercritical region. In addition, they proposed a new mixing rule for predicting the properties of mixtures.[60] Combined with their proposed mixing rule, their cubic EOS can accurately describe the phase equilibria of polar/non-polar systems. The pressure was set to 280 bar and the temperature to 650 °C (as set in the experiments). The feed has a temperature of 20 °C. x_c^* was varied from 0.001 to 8.0 mol/mol (see Figure 11). The

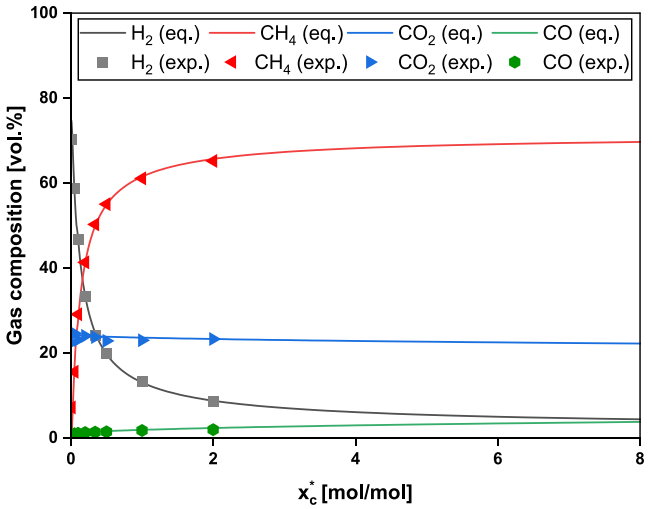

Figure 11. Comparison of experimentally measured (exp.) and simulated gas composition (eq.) for different x_c^* values in the feed solution.

simulation verified the results from Voll et al., who calculated the thermodynamic equilibrium of the SCWG of ethanol at 800 °C and 221 bar.[49] It was found that the simulation produced accurately their results (see Supporting Information Figure S1).

The results indicate that in the present reaction system under the chosen reaction conditions, thermodynamic equilibrium is reached for x_c^* greater than 0.05 (see Figure 11). Potassium has played a crucial role in achieving equilibrium. This becomes clear when comparing the gas composition acquired when the reaction system was newly implemented (experiment 1) with the calculated gas composition (see Table 7). With the newly implemented reaction system, far less H_2 and more CH_4 was produced. Additionally, experiments showed that coke and many hydrocarbons formed in the new reaction system. Without the presence of potassium, the dehydration pathway of ethanol decomposition, which leads to hydrocarbons,[32] seems to be favored, instead of the dehydrogenation pathway, which mainly leads to H_2 and CO_2. This emphasizes the influence of potassium as a homogeneous catalyst in the present system.

According to Aspen HYSYS at x_c^* = 0.08, the gas composition is (almost) exactly the composition described by eq 26 (24.2 vol % CO_2, 50.1 vol % H_2, 24.6 vol % CH_4), and the water consumption is close to 1 (0.96). At this point, the gas composition can be explained by the ethanol decomposition. For lower x_c^* than 0.08, less methane should be in the product gas than the amount formed according to eq 26. This means that steam methane reforming needs to take place to reach equilibrium. Experimental results show that even though it is true that less methane is in the product gas than the amount that forms according to eq 26 (see Table 5), methane is not completely reformed to reach equilibrium. In the case of x_c^* = 0.05, equilibrium is reached (see Table 7), but for x_c^* = 0.01, the experimental results indicate a higher methane content (7.1 vol %) than that predicted by Aspen HYSYS (0.8 vol %). More catalytically active sites are needed to reach equilibrium. Steam methane reforming is often promoted on nickel-based catalysts with a high surface area.[61] Thus, the methane content is higher than that predicted by the equilibrium. For x_c^* higher than 0.08, the amount of methane in the product gas can be explained by considering methanation. Since equilibrium is reached in these cases, methanation can be considered to take place completely.

Besides the gas compositions (see Figure 12), the water consumption determined by Aspen HYSYS also fits the

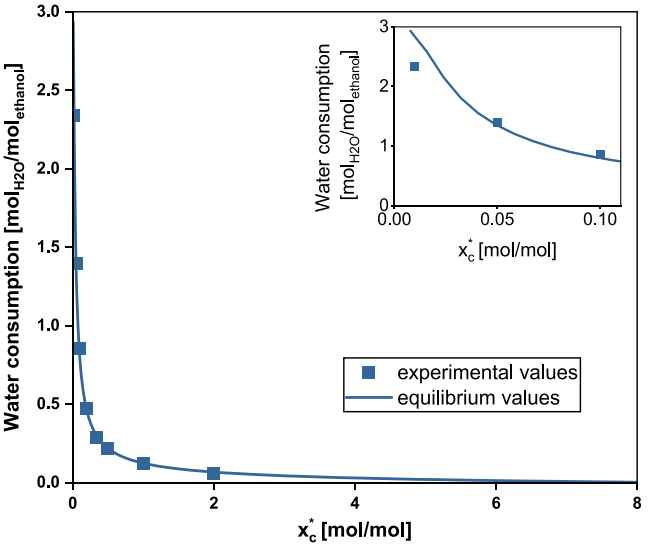

Figure 12. Comparison of experimentally measured (exp.) and simulated (eq.) water consumption for different x_c^* values.

experimental data well (see Figure 13). The deviation is smaller than 0.04 mol/mol for x_c^* greater than 0.05. The deviation is more prominent in the case of x_c^* = 0.01, but the general trend is still visible. This deviation is due to the deviation in gas compositions as described above. To emphasize the overall accuracy of the simulation with the experiments, the parity plot of the water consumption calculated by Aspen HYSYS and from experimental data is

Table 7. Influence of Catalyst on Reaching the Equilibrium Comparing Experimental Gas Compositions with Aspen Simulation

Exp. Nr.	catalyst	x_c^* (mol/mol)	H_2 (vol %)	CO (vol %)	CO_2 (vol %)	CH_4 (vol %)	C_{2+} (vol %)
1		0.05	37.2	11.9	14.8	27.9	8.2
4	$KHCO_3$	0.05	58.8	1.0	24.5	15.6	0.1
Aspen		0.05	58.0	1.0	24.0	17.0	0.0

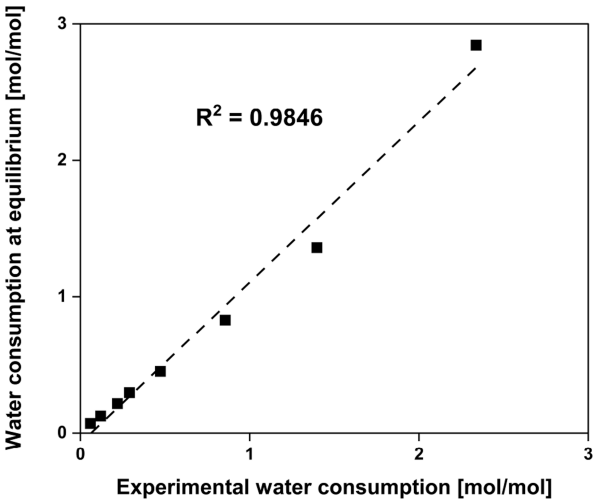

Figure 13. Parity plot of water consumption experimentally determined and simulated by ASPEN.

shown (see Figure 13). The coefficient of determination R^2 is 0.985, which is very close to 1 (= ideal concordance). This confirms the chosen calculation method for the water consumption based on the experimentally acquired gas compositions.

The simulation of thermodynamic equilibrium with Aspen HYSYS is helpful for determining further reaction parameters that could be investigated. A further extension of residence time would in this case probably not change the outcome of the experiments since under the chosen residence, time equilibrium gas composition was reached.

4. SUMMARY

The water consumption of the supercritical water gasification of ethanol was systematically investigated and described since a higher water consumption that results in higher hydrogen generation is an important factor for SCWG. It was demonstrated that the water consumption of the supercritical water gasification of ethanol can be reliably calculated using the composition of the produced gas. The calculation was supported by ASPEN HYSYS simulations of the investigated process. The gas composition and the water consumption strongly depend on the ethanol concentration in the feed. With rising ethanol concentration, the water consumption of the process decreases in a logarithmic manner. This is due to increased methanation, which produces water as a side product. Simple equations were derived, which enable the calculation of the water consumption of the process. Furthermore, the influence of potassium as a homogeneous catalyst on the coke formation, gasification efficiency, and the ability to reach thermodynamic equilibrium was demonstrated. With potassium as a catalyst, thermodynamic equilibrium was reached under the chosen reaction conditions (T = 650 °C, p = 280 bar, τ = 3 min) for ethanol concentrations between 6 and 72 wt %. In the future, the water consumption should be measured for complex biomasses like lignocelluloses to extend the knowledge. The influence of other process parameters like reaction temperature or system pressure on this key figure should also be investigated.

■ ASSOCIATED CONTENT

● Supporting Information

The Supporting Information is available free of charge at https://pubs.acs.org/doi/10.1021/acs.iecr.3c01595.

Additional experimental details (pH values of the liquid effluents) and Aspen HYSYS model validation (PDF)

■ AUTHOR INFORMATION

Corresponding Author

Julian Dutzi − *Institute of Catalysis Research and Technology (IKFT), Karlsruhe Institute of Technology (KIT), 76344 Eggenstein-Leopoldshafen, Germany;* orcid.org/0000-0001-7584-0467; Phone: +49-721-6082-8813; Email: julian.dutzi@kit.edu

Authors

Athanasios A. Vadarlis − *Institute of Catalysis Research and Technology (IKFT), Karlsruhe Institute of Technology (KIT), 76344 Eggenstein-Leopoldshafen, Germany*

Nikolaos Boukis − *Institute of Catalysis Research and Technology (IKFT), Karlsruhe Institute of Technology (KIT), 76344 Eggenstein-Leopoldshafen, Germany*

Jörg Sauer − *Institute of Catalysis Research and Technology (IKFT), Karlsruhe Institute of Technology (KIT), 76344 Eggenstein-Leopoldshafen, Germany;* orcid.org/0000-0003-3133-4110

Author Contributions

Conceptualization, J.D., A.V., and N.B.; methodology, N.B.; validation, J.D., A.V., N.B., and J.S.; formal analysis, J.D. and A.V.; investigation, J.D. and A.V.; resources, N.B.; data curation, J.D. and A.V.; writing—original draft preparation, J.D. and A.V.; writing—review and editing, N.B. and J.S.; visualization, J.D. and A.V.; supervision, J.S.; All authors have read and agreed to the published version of the manuscript.

Notes

The authors declare no competing financial interest.

■ ACKNOWLEDGMENTS

The authors would like to thank Mrs. E. Hauer for the contributions to the experimental work and Mr. K. Weiss, responsible for most of the mechanical work, for his contributions.

■ REFERENCES

(1) Kaltschmitt, M.; Hartmann, H.; Hofbauer, H. *Energie aus Biomasse*, 2nd ed.; Springer, 2009, DOI: 10.1007/978-3-540-85095-3.

(2) Kruse, A.; Dinjus, E. Hot compressed water as reaction medium and reactant properties and synthesis reactions. *J. Supercrit. Fluids* **2007**, *39*, 362−380.

(3) Boukis, N.; Galla, U.; Müller, H.; Dinjus, E. Biomass Gasification in Supercritical Water. Experimental progress achieved with the VERENA pilot plant. In *Proceedings of 15th European Biomass Conference & Exhibition*, Berlin, Germany, 7−11 May 2007; pp. 1013-1016.

(4) Boukis, N.; Galla, U.; Diem, V.; D'Jesus, P.; Dinjus, E. Hydrogen production from biomass in supercritical water. In *Proceedings of H2-age: When, Where, Why*, Pisa, Italy, 16−19 May 2004.

(5) Boukis, N.; Diem, V.; Dinjus, E.; Galla, U.; Kruse, A. Biomass Gasification in Supercritical Water. In *Proceedings of 12th European*

Conference on Biomass for Energy, Industry and Climate Protection, Amsterdam, Netherlands, 17−21 June 2002.
(6) Demirbas, A. Hydrogen-rich gas from fruit shells via supercritical water extraction. *Int. J. Hydrogen Energy* **2004**, *29*, 1237−1243.
(7) Peterson, A. A.; Vogel, F.; Lachance, R. P.; Fröling, M.; Antal, M. J., Jr.; Tester, J. W. Thermochemical biofuel production in hydrothermal media: A review of sub- and supercritical water technologies. *Energy Environ. Sci.* **2008**, *1*, 32−65.
(8) Lee, C. S.; Conradie, A. V.; Lester, E. Review of supercritical water gasification with lignocellulosic real biomass as the feedstocks: Process parameters, biomass composition, catalyst development, reactor design and its challenges. *Chem. Eng. J.* **2021**, *415*, No. 128837.
(9) Resende, F. L. P.; Savage, P. E. Kinetic Model for Noncatalytic Supercritical Water Gasification of Cellulose and Lignin. *AIChE J.* **2010**, *56*, 2412−2420.
(10) Waldner, M. H.; Vogel, F. Renewable Production of Methane from Woody Biomass by Catalytic Hydrothermal Gasification. *Ind. Eng. Chem. Res.* **2005**, *44*, 4543−4551.
(11) Guan, Q.; Wei, C.; Savage, P. E. Kinetic model for supercritical water gasification of algae. *Phys. Chem. Chem. Phys.* **2012**, *14*, 3140−3147.
(12) Kruse, A.; Funke, A.; Titirici, M.-M. Hydrothermal conversion of biomass to fuels and energetic materials. *Curr. Opin. Biotechnol.* **2013**, *17*, 515−521.
(13) Susanti, R. F.; Veriansyah, B.; Kim, J.-D.; Kim, J.; Lee, Y.-W. Continuous supercritical water gasification of isooctane: A promising reactor design. *Int. J. Hydrogen Energy* **2010**, *35*, 1957−1970.
(14) Boukis, N.; Stoll, I. K. Gasification of Biomass in Supercritical Water, Challenges for the Process Design—Lessons Learned from the Operation Experience of the First Dedicated Pilot Plant. *Processes* **2021**, *9*, 455.
(15) Boukis, N.; Galla, U.; D'Jesús, P.; Müller, H.; Dinjus, E. Gasification of wet biomass in supercritical water. Results of pilot plant experiments. In *Proceedings of 14th European Biomass Conference for Energy, Industry and Climate Protection*, Paris, France, 17−21 October 2005.
(16) Rodriguez Correa, C.; Kruse, A. Supercritical water gasification of biomass for hydrogen production − Review. *J. Supercrit. Fluids* **2018**, *133*, 573−590.
(17) Gadhe, J. B.; Gupta, R. B. Hydrogen Production by Methanol Reforming in Supercritical Water: Suppression of Methane Formation. *Ind. Eng. Chem. Res.* **2005**, *44*, 4577−4585.
(18) Savage, P. E. A perspective on catalysis in sub- and supercritical water. *J. Supercrit. Fluids* **2009**, *47*, 407−414.
(19) Okolie, J. A.; Rana, R.; Nanda, S.; Dalai, A. K.; Kozinski, J. A. Supercritical water gasification of biomass: a state-of- the-art review of process parameters, reaction mechanisms and catalysis. *Sustainable Energy Fuels* **2019**, *3*, 578−598.
(20) Nanda, S.; Reddy, S. N.; Hunter, H. N.; Dalai, A. K.; Kozinski, J. A. Supercritical water gasification of fructose as a model compound for waste fruits and vegetables. *J. Supercrit. Fluids* **2015**, *104*, 112−121.
(21) D'Jesus, P. Die Vergasung von realer Biomasse in überkritischem Wasser:Untersuchung des Einflusses von Prozessvariablen und Edukteigenschaften. Dissertation, Universität Karlsruhe, 2007.
(22) Brandenberger, M.; Matzenberger, J.; Vogel, F.; Ludwig, C. Producing synthetic natural gas from microalgae via supercritical water gasification: A techno-economic sensitivity analysis. *Biomass Bioenergy* **2013**, *51*, 26−34.
(23) Chen, J.; Liang, J.; Xu, Z.; Jiaqiang, E. Assessment of supercritical water gasification process for combustible gas production from thermodynamic, environmental and techno-economic perspectives: A review. *Energy Convers. Manage.* **2020**, *226*, No. 113497.
(24) Fiori, L.; Valbusa, M.; Castello, D. Supercritical water gasification of biomass for H2 production: Process design. *Bioresour. Technol.* **2012**, *121*, 139−147.
(25) Wang, T.; Liu, X.; Liu, H.; He, M. Synergistic effect of supercritical water and nanocatalyst on lignin gasification. *Int. J. Hydrogen Energy* **2021**, *46*, 34626−34637.
(26) D'Jesús, P.; Boukis, N.; Kraushaar-Czarnetzki, B.; Dinjus, E. Gasification of corn and clover grass in supercritical water. *Fuel* **2006**, *85*, 1032−1038.
(27) Akgül, G.; Kruse, A. Influence of salts on the subcritical water-gas shift reaction. *J. Supercrit. Fluids* **2012**, *66*, 207−214.
(28) Boukis, N.; Habicht, W.; Hauer, E.; Weiss, K.; Dinjus, E. Corrosion behavior of Ni-base alloy 625 in supercritical water containing alcohols and potassium hydrogen carbonate. In *the Proceedings of EUROCORR 2007 the European Corrosion Congress*, Freiburg in Breisgau, Germany, September 9−13, 2007.
(29) Habicht, W.; Boukis, N.; Hauer, E.; Dinjus, E. Analysis of hydrothermally formed corrosion layers in Ni-base alloy 625 by combined FE-SEM and EDXS. *X-Ray Spectrom.* **2011**, *40*, 69−73.
(30) Dutzi, J.; Boukis, N.; Sauer, J. Process Effluent Recycling in the Supercritical Water Gasification of Dry Biomass. *Processes* **2023**, *11*, 797.
(31) Boukis, N.; Diem, V.; Habicht, W.; Dinjus, E. Methanol Reforming in Supercritical Water. *Ind. Eng. Chem. Res.* **2003**, *42*, 728−735.
(32) Arita, T.; Nakahara, K.; Nagami, K.; Kajimoto, O. Hydrogen generation from ethanol in supercritical water without catalyst. *Tetrahedron Lett.* **2003**, *44*, 1083−1086.
(33) Diem, V.; Boukis, N.; Hauer, E.; Franz, G.; Dinjus, E. Reaction Of Alcohols With Supercritical Water. In *Proceedings of 7th Italian Conference on Supercritical Fluids and Their Applications*, Trieste, Italy, June 2004; pp. 13−16.
(34) Therdthianwong, S.; Srisiriwat, N.; Therdthianwong, A.; Croiset, E. Hydrogen production from bioethanol reforming in supercritical water. *J. Supercrit. Fluids* **2011**, *57*, 58−65.
(35) Zeebe, R. E.; Wolf-Gladrow, D. *CO2 in Seawater: Equilibrium, Kinetics, Isotopes*; Elsevier Science, 2001.
(36) Sınağ, A.; Kruse, A.; Schwarzkopf, V. Key Compounds of the Hydropyrolysis of Glucose in Supercritical Water in the Presence of K2CO3. *Ind. Eng. Chem. Res.* **2003**, *42*, 3516−3521.
(37) Kruse, A.; Faquir, M. Hydrothermal Biomass Gasification − Effects of Salts, Backmixing, and Their Interaction. *Chem. Eng. Technol.* **2007**, *30*, 749−754.
(38) Kruse, A.; Meier, D.; Rimbrecht, P.; Schacht, M. Gasification of Pyrocatechol in Supercritical Water in the Presence of Potassium Hydroxide. *Ind. Eng. Chem. Res.* **2000**, *39*, 4842−4848.
(39) Muangrat, R.; Onwudili, J. A.; Williams, P. T. Alkali-promoted hydrothermal gasification of biomass food processing waste: A parametric study. *Int. J. Hydrogen Energy* **2010**, *35*, 7405−7415.
(40) Onwudili, J. A.; Lea-Langton, A. R.; Ross, A. B.; Williams, P. T. Catalytic hydrothermal gasification of algae for hydrogen production: Composition of reaction products and potential for nutrient recycling. *Bioresour. Technol.* **2013**, *127*, 72−80.
(41) Xu, Z. R.; Zhu, W.; Gong, M.; Zhang, H. W. Direct gasification of dewatered sewage sludge in supercritical water. Part 1: Effects of alkali salts. *Int. J. Hydrogen Energy* **2013**, *38*, 3963−3972.
(42) Habicht, W.; Boukis, N.; Franz, G.; Dinjus, E. Investigation of Nickel-Based Alloys Exposed to Supercritical Water Environments. *Microchim. Acta* **2004**, *145*, 57−62.
(43) Habicht, W.; Boukis, N.; Dinjus, E. Surface analysis by FESEM/EDX of alloy 625 exposed to supercritical water containing KHCO3. In *the Proceedings of 8th Multinational Congress on Microscopy*, Prague, Czech Republic, 17−21 June 2007.
(44) Habicht, W.; Boukis, N.; Hauer, E.; Dinjus, E. Studies on hydrothermally grown corrosion layers by FESEM/EDX and AFM. In *the Proceedings of 8th Internat.Conf.on Electron Microscopy*, Zakopane, PL, June 8−11, 2008.
(45) Boukis, N.; Habicht, W.; Franz, G.; Dinjus, E. Behavior of alloy 625 as reactor material for methanol conversion in supercritical water. In *the Proceedings of 15th International Corrosion Congress, Frontiers in Corrosion Science and Technology*, Granada ,Spain, September 22 to 27, 2002.

(46) Boukis, N.; Habicht, W.; Hauer, E.; Weiss, K.; Dinjus, E. Corrosion Behavior of Ni-Base Alloys and Stainless Steels in Supercritical Water Containing Potassium Hydrogen Carbonate. In *Proceedings of the EUROCORR 2008: The European Corrosion Congress*, Edinburgh, United Kingdom, 7 September 2008.
(47) Boukis, N.; Hauer, E.; Habicht, W. Corrosion Behaviour of Ni-Base Alloys in Supercritical Water Containing Alkali Chlorides. In *Proceedings of the EUROCORR 2013*: The European Corrosion Congress, Estoril, Portugal, 2 September 2013.
(48) Byrd, A. J.; Pant, K. K.; Gupta, R. B. Hydrogen Production from Ethanol by Reforming in Supercritical Water Using Ru/Al2O3 Catalyst. *Energy Fuels* **2007**, *21*, 3541−3547.
(49) Voll, F. A. P.; Rossi, C. C. R. S.; Silva, C.; Guirardello, R.; Souza, R. O. M. A.; Cabral, V. F.; Cardozo-Filho, L. Thermodynamic analysis of supercritical water gasification of methanol, ethanol, glycerol, glucose and cellulose. *Int. J. Hydrogen Energy* **2009**, *34*, 9737−9744.
(50) Chen, G.; Andries, J.; Luo, Z.; Spliethoff, H. Biomass pyrolysis/gasification for product gas production: the overall investigation of parametric effects. *Energy Convers. Manage.* **2003**, *44*, 1875−1884.
(51) Yakaboylu, O.; Albrecht, I.; Harinck, J.; Smit, K. G.; Tsalidis, G.-A.; Di Marcello, M.; Anastasakis, K.; de Jong, W. Supercritical water gasification of biomass in fluidized bed: First results and experiences obtained from TU Delft/Gensos semi-pilot scale setup. *Biomass Bioenergy* **2018**, *111*, 330−342.
(52) Lee, I.-G.; Kim, M.-S.; Ihm, S.-K. Gasification of Glucose in Supercritical Water. *Ind. Eng. Chem. Res.* **2002**, *41*, 1182−1188.
(53) Lu, Y. J.; Guo, L. J.; Ji, C. M.; Zhang, X. M.; Hao, X. H.; Yan, Q. H. Hydrogen production by biomass gasification in supercritical-water: A parametric study. *Int. J. Hydrogen Energy* **2006**, *31*, 822−831.
(54) Promdej, C.; Matsumura, Y. Temperature Effect on Hydrothermal Decomposition of Glucose in Sub- And Supercritical Water. *Ind. Eng. Chem. Res.* **2011**, *50*, 8492−8497.
(55) Demirbaş, A. Biomass resource facilities and biomass conversion processing for fuels and chemicals. *Energy Convers. Manage.* **2001**, *42*, 1357−1378.
(56) Nanda, S.; Rana, R.; Hunter, H. N.; Fang, Z.; Dalai, A. K.; Kozinski, J. A. Hydrothermal catalytic processing of waste cooking oil for hydrogen-rich syngas production. *Chem. Eng. Sci.* **2019**, *195*, 935−945.
(57) Nanda, S.; Gong, M.; Hunter, H. N.; Dalai, A. K.; Gökalp, I.; Kozinski, J. A. An assessment of pinecone gasification in subcritical, near-critical and supercritical water. *Fuel Process. Technol.* **2017**, *168*, 84−96.
(58) Reddy, S. N.; Nanda, S.; Dalai, A. K.; Kozinski, J. A. Supercritical water gasification of biomass for hydrogen production. *Int. J. Hydrogen Energy* **2014**, *39*, 6912−6926.
(59) Yu, D.; Aihara, M.; Antal, M. J., Jr. Hydrogen Production by Steam Reforming Glucose in Supercritical Water. *Energy Fuels* **1993**, *7*, 574−577.
(60) Twu, C. H.; Bluck, D.; Cunningham, J. R.; Coon, J. E. A cubic equation of state with a new alpha function and a new mixing rule. *Fluid Phase Equilib.* **1991**, *69*, 33−50.
(61) Fowles, M.; Carlsson, M. Steam Reforming of Hydrocarbons for Synthesis Gas Production. *Top. Catal.* **2021**, *64*, 856−875.